Supplementary Information

Binary carbon@silica@carbon hydrophobic nanoreactor for highly efficient selective oxidation of aromatic alkanes

Ganghua Xiang,[a] Lushuang Zhang, [a] Junnan Chen, [b] Bingsen Zhang[b] and Zhigang Liu*[a]*

[a] Engineering Research Center of Advanced Catalysis of Ministry of Education, College of Chemistry and Chemical Engineering, Hunan University, Changsha, Hunan, 410082, China. E-mail: liuzhigang@hnu.edu.cn

[b] Shenyang National Laboratory for Materials Science, Institute of Metal Research, Chinese Academy of Sciences, Shenyang, Liaoning, 110016, China. E-mail: bszhang@imr.ac.cn

Number of pages: 5

Number of figures: 2

Number of tables: 5

E-mail: liuzhigang@hnu.edu.cn (Z. Liu); bszhang@imr.ac.cn (B. Zhang).

Characterization

Using a NOVA 1000e from Quantachrome Instruments, N_2 adsorption-desorption analysis of the samples outgassed at 200 ℃ for 3 h were conducted at -196 ℃ and the relative pressure ranging from 0.05 to 0.98. The specific surface areas were calculated using the BET method. The pore size distribution plot was recorded from the desorption branch of the isotherm based on the BJH model. The TEM and the high angle annular dark field scanning TEM images (HAADF-STEM) were obtained on an FET Tecnai G 2 F20 operating at 200 kV. The X-ray powder diffraction (XRD) was performed on a Bruker D8 Advance analyzer with Ni-filtered Cu Kα radiation (40 kV, 40 mA). Raman was analyzed on a Mono Vista 2560 Spectrometer with a laser at 532 nm (2.33 eV). X-ray photoelectron spectra (XPS) measurements were taken on an Escalab 520Xi system using Al Kα radiation (1486.6 eV).

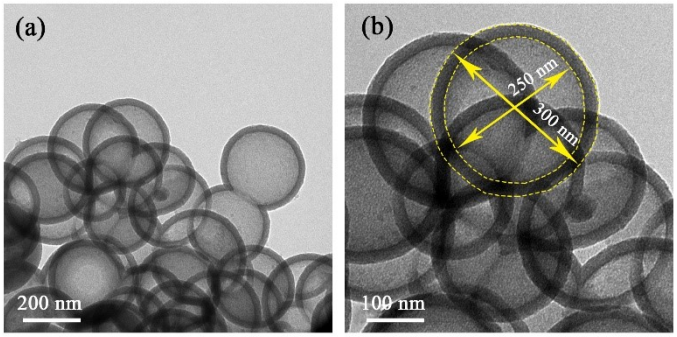

Fig S1. (a-b) Low-magnification TEM image of $mSiO_2$.

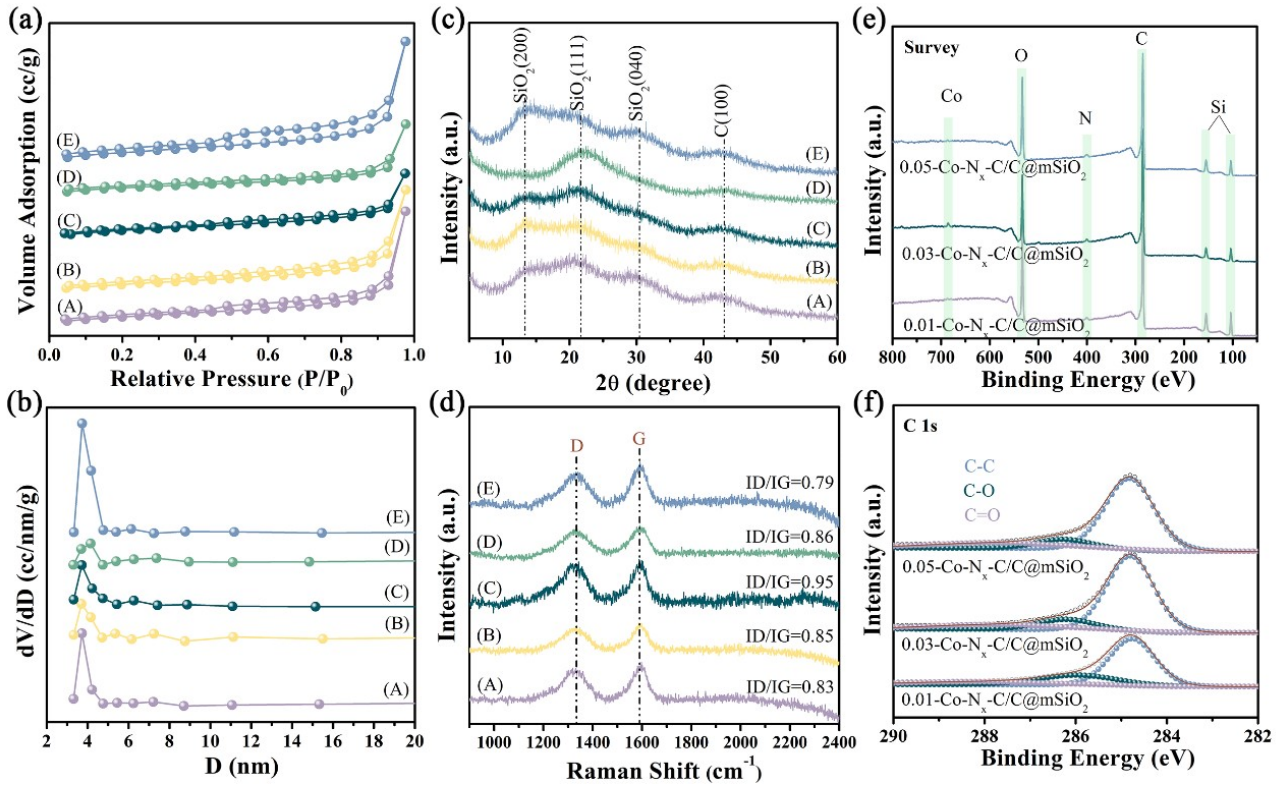

Fig S2. (a) The nitrogen adsorption-desorption isotherms, (b) the pore size distribution curves calculated on the basis of the BJH equation, (c) XRD patterns and (d) Raman spectra of (A) 0.01-Co-N_x-C/C@$mSiO_2$, (B) 0.02-Co-N_x-C/C@$mSiO_2$, (C) 0.03-Co-N_x-C/C@$mSiO_2$, (D) 0.04-Co-N_x-C/C@$mSiO_2$ and (E) 0.05-Co-N_x-C/C@$mSiO_2$; (e) Survey spectra and (f) C 1s high-resolution XPS spectra of 0.01-Co-N_x-C/C@$mSiO_2$, 0.03-Co-N_x-C/C@$mSiO_2$ and 0.05-Co-N_x-C/C@$mSiO_2$.

Table S1. Nitrogen adsorption and desorption test data.

Entry	Sample	S_{BET} (m^2/g)	D_p (nm)	V_p (cm^3/g)
1	$mSiO_2$	481	6.08	0.73
2	0.03-Co-N_x-C/C@$mSiO_2$	151	8.23	0.17
3	0.03-Co-N_x-C/C@SiO_2	45	4.76	0.05
4	0.03-Co-N_x-C/SiO_2@$mSiO_2$	170	7.83	0.33
5	0.01-Co-N_x-C/C@$mSiO_2$	103	9.00	0.23
6	0.02-Co-N_x-C/C@$mSiO_2$	105	8.94	0.19
7	0.04-Co-N_x-C/C@$mSiO_2$	154	7.10	0.11
8	0.05-Co-N_x-C/C@$mSiO_2$	165	6.34	0.28
9	0.03-Co-N_x-C/C@$mSiO_2$-R	131	7.52	0.25

Table S2. The valence state composition of Co and N elements on 0.01-Co-N_x-C/C@$mSiO_2$, 0.03-Co-N_x-C/C@$mSiO_2$, 0.05-Co-N_x-C/C@$mSiO_2$ and 0.03-Co-N_x-C/C@$mSiO_2$-R by XPS analysis.

Sample	N/at%				Co/at%	
	Co-N_x	Pyrrole-N	Graphite-N	N-Oxide	Co	Co-N_x
0.01-Co-N_x-C/C@$mSiO_2$	23.4	-	63.3	13.3	11.5	88.5
0.03-Co-N_x-C/C@$mSiO_2$	39.8	2.0	27.9	30.3	-	100
0.05-Co-N_x-C/C@$mSiO_2$	27.1	11.7	34.4	26.8	12.4	87.6
0.03-Co-N_x-C/C@$mSiO_2$-R	37.2	-	35.7	27.1	12.7	87.3

Table S3. The content table of C, O, N, Co, Si elements of different catalysts.

sample	C/at%	O/at%	N/at%	Si/at%	Co/at%
0.01-Co-N_x-C/C@$mSiO_2$	64.3	22.5	1.3	11.7	0.2
0.03-Co-N_x-C/C@$mSiO_2$	75.0	15.5	1.8	7.4	0.3
0.05-Co-N_x-C/C@$mSiO_2$	71.6	18.2	1.7	8.2	0.3
0.03-Co-N_x-C/C@$mSiO_2$-R	75.5	15.1	1.5	7.7	0.2

Table S4. The mass fraction of Co element from XPS analysis and ICP

sample	XPS/wt%	ICP/wt%
0.03-Co-N_x-C/C@ $mSiO_2$	1.3	1.7

Table S5. Catalytic performance comparison of catalysts reported before in the literatures.

Materials	Solvent	Oxidant (Molar ratio of ethylbenzene: oxidant)	T (°C)	Time (h)	Yield (%)	Ref.
Mn-ZSM-5-50	H_2O and acetonitrile	TBHP (1 : 3)	80	6	90	[1]
Fe_3O_4 nanoparticles	none	TBHP (1 : 2)	120	2	95	[2]
GS1000 nanosheets	H_2O	TBHP (1 : 10.5)	80	4	85	[3]
CZD650	H_2O	TBHP (1 : 3)	80	4	78	[4]
GNMC	acetonitrile	TBHP (1 : 3)	80	12	80	[5]
Pd/g-C_3N_4–rGO	acetonitrile	TBHP (1 : 4)	80	24	92	[6]
NS-CSs	H_2O	TBHP (1 : 3)	80	10	94	[7]
Co-Cu/SAPS-15	none	TBHP (1 : 3)	80	6	64	[8]
Co-Cu/SAPS-15	none	TBHP (1 : 3)	100	6	96	[8]

Reference

[1] X. Liu, S. Gao, F. Yang, S. Zhou, Y. Kong, Research on Chemical Intermediates, 46 (2020) 2817–2832.

[2] M. Zarghani, B. Akhlaghinia, RSC Adv., 6 (2016) 38592-38601.

[3] X. Hu, Y. Liu, H. Huang, B. Huang, G. Chai and Z. Xie, Green Chem., 2020, 22, 1291–1300.

[4] M. Nandi, A.K. Talukdar, Arabian Journal of Chemistry (2019) 12, 3753–3763.

[5] J. Wang, X. Pan and F. Li, RSC Adv., 2019, 9, 28253.

[6] S. Nilforoushan, M. Ghiaci, S. M. Hosseini, S. Laurent and R. N. Muller, New J. Chem., 2019, 43, 6921.

[7] M. Liu, Y. Liu, Z. Gao, C. Wang, W. Ye, R. Lu and S. Zhang, New J. Chem., 2018, 42, 15962.

[8] V. Chaudhary, S. Sharma, Asia-Pac J Che m Eng. 2020;15: e2441.